Critical Scenario Generation for Signalized Intersections via Liouville Guided Temporal Reparameterization

Anonymous ECCV 2026 Submission

Paper ID #*****

Abstract. Autonomous driving evaluation at signalized intersections is particularly demanding because road users interact under dense traffic, signal control, and right of way constraints. Since hazardous interactions occur infrequently in naturalistic data, existing datasets provide limited support for constructing realistic critical scenario libraries. We therefore formulate critical scenario generation as the controlled evolution of recorded interactions in a compact conflict state space. The state jointly captures the arrival time gap at the conflict point and the minimum spatial clearance, while a phase conditioned potential integrates empirical statistics, shrinkage estimation, and a structural risk prior. The normalized potential gradient defines the characteristic direction of increasing criticality, and the Liouville continuity equation describes the corresponding evolution at the population level. Individual variants are then realized through temporal reparameterization along the recorded paths. Results on the SinD dataset demonstrate controllable progression toward more critical surrogate states without altering the original path geometry.

Keywords: Autonomous vehicle · Scenario generation · Signalized intersection · Risk evolution

1 Introduction

Signalized intersections are challenging environments for autonomous driving evaluation because road users interact under conflicting motion intentions, traffic signal control, and narrow safety margins [1]. Small behavioral changes can therefore produce substantially different outcomes. Reliable evaluation requires diverse scenarios that cover routine and critical interactions, yet hazardous events are rare in naturalistic trajectory data [2].

Interaction criticality depends jointly on temporal coordination, spatial separation, path conflicts, and signal conditions [3]. Conventional surrogate measures, such as time to collision and post encroachment time, usually capture only one aspect of an interaction. A small arrival gap may remain safe when sufficient clearance is maintained, whereas a small clearance may be benign when participants traverse the conflict region at different times [4]. Similar trajectories can also have different safety implications under different signal phases. A signal dependent representation that combines temporal and spatial margins is therefore needed.

Existing generation methods do not fully meet this requirement. Surrogate measures can identify critical interactions but provide limited guidance on how a recorded scenario should be modified [5]. Heuristic perturbations are difficult to control systematically, while unconstrained data driven methods may alter route geometry, maneuver semantics, or conflict structure [6]. It then becomes unclear whether increased criticality results from temporal coordination or from a different interaction.

We address this gap by formulating critical scenario generation as the controlled evolution of recorded interactions. Road geometry, vehicle paths, maneuver types, and conflict relations are preserved, while timing near the conflict region is adjusted. Each interaction is represented by the arrival time gap and minimum spatial clearance. A signal phase conditioned potential is estimated from SinD trajectories through empirical smoothing, global shrinkage, and a structural prior. Its gradient defines a direction of increasing criticality, while the Liouville formulation describes population transport. Temporal reparameterization along the recorded paths then realizes the desired evolution.

The main contributions are:

- We introduce a signal aware interaction representation that combines the arrival time gap and minimum vehicle clearance, together with a phase conditioned potential that captures variation across signal conditions.
- We formulate scenario generation as continuous evolution in the conflict state space, where the potential gradient defines an interpretable characteristic field and the Liouville formulation provides a population level transport interpretation.
- We develop a path constrained temporal reparameterization method that generates feasible variants while preserving geometry, paths, maneuver semantics, and conflict relations.

Fig. 1 illustrates how the proposed framework transforms a recorded intersection interaction into a more critical yet source consistent scenario variant. First, recorded trajectories, conflict geometry, and synchronized signal states are used to extract an interacting vehicle pair and represent it by the conflict

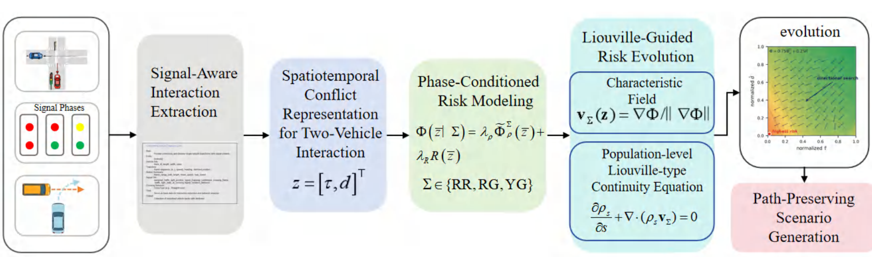

Fig. 1: Overall framework for signal conditioned risk evolution and path preserving critical scenario generation. Recorded interactions are mapped into a compact conflict state space, where a phase conditioned potential and its characteristic field determine the direction of increasing criticality. The resulting state displacement is realized through temporal reparameterization along the recorded paths.

state $\mathbf{z} = [\tau, d]^\top$, where τ and d describe the temporal separation and minimum spatial clearance near the conflict point. A signal phase conditioned potential Φ is then constructed from empirical interaction statistics, shrinkage toward a global estimate, and a structural risk prior. Its normalized gradient defines the characteristic direction toward states with higher potential, while the Liouville continuity equation provides a population level interpretation of the corresponding state transport. Finally, the desired displacement in conflict space is mapped back to trajectory space through temporal reparameterization along the recorded paths. This process preserves road geometry, maneuver semantics, and conflict relations, while adjusting conflict region occupancy to generate traceable and controllably more critical interaction scenarios.

2 Related Work

2.1 Surrogate Criticality Measures for Intersection Conflicts

Traffic conflict analysis supports proactive safety evaluation when crash observations are sparse. Common surrogate measures include time to collision, post encroachment time, arrival gaps, deceleration indicators, and minimum distances [7,8]. Time based measures describe temporal proximity or conflict region occupancy, whereas distance based measures capture spatial separation. Their interpretation depends on road geometry, maneuver type, vehicle dimensions, and operational context [8, 9].

At signalized intersections, criticality also depends on signal phases and right of way allocation. A single temporal or spatial measure may therefore be insufficient. A small arrival gap does not necessarily imply inadequate clearance, while a small distance may remain safe when participants cross at different times. We therefore represent each interaction through the arrival time gap and minimum vehicle clearance under the corresponding signal condition.

2.2 Interaction Modeling and Controllable Traffic Generation

Recent trajectory prediction methods increasingly model interactions among multiple participants. QCNet uses query centered representations [10], MotionLM models joint futures autoregressively [11], and GameFormer introduces hierarchical game theoretic reasoning [12]. Other work addresses local interaction density [13], while SinD and INT2 provide signal annotated intersection trajectories [6, 14]. These methods improve motion prediction but do not explicitly evolve recorded interactions toward greater criticality.

Controllable generation methods provide greater flexibility. Scenario Diffusion uses map and control conditions [15], InteractTraj converts language descriptions into trajectories [16], and BehaviorGPT simulates multiagent behavior autoregressively [17]. ScenarioNet supports large scale traffic reconstruction [18], while ChatScene combines language instructions with domain knowledge [19]. Gu et al. [20] develop a signal conditioned imitation learning framework for SinD.

These methods improve realism, diversity, or controllability, but global generation may alter route geometry, maneuver semantics, or conflict structure. Our method instead preserves recorded paths and conflict relations while modifying only temporal coordination near the conflict region.

2.3 Critical Scenario Mutation and Risk Guided Search

Critical scenario generation commonly uses adversarial testing, rare event simulation, parameter search, and perturbation of recorded or simulated scenarios [21]. These methods search for states or parameters that reduce safety margins. However, optimization in the original scenario space may offer limited insight into how criticality changes, and unconstrained perturbations may produce unrealistic motions or alter the original conflict structure.

Recorded scenario mutation preserves observed geometry and maneuver semantics [6], but heuristic changes in speed, acceleration, or arrival time do not define a continuous and signal dependent direction of increasing criticality [14]. Existing work also provides limited guidance for mapping a desired risk change to feasible trajectories. We address this gap by constructing a signal phase conditioned potential in a joint temporal and spatial state space and realizing its gradient direction through temporal reparameterization along the recorded paths.

3 Method

3.1 Overview and Signal Aware Interaction Representation

We extract interacting vehicle pairs from SinD and associate each vehicle with traffic light semantics using map geometry and timestamps. Raw phases are mapped to red, green, yellow, or unknown. Retained interactions are grouped as RR(Red light-Red light), RG(Red light-Green light), and YG(Yellow light-Green light), denoting red and red, red and green, and yellow and green combinations. Other combinations are excluded from phase specific estimation but may contribute to the global estimate.

Fig. 2 illustrates the geometric quantities. Intersecting paths define a conflict point, but risk is evaluated from time indexed vehicle boxes within a local window. This prevents geometrically crossing paths from being labeled critical when the vehicles pass at different times.

Each interaction is represented by $z = [\tau, d]^\top$, where τ is the arrival time gap at the conflict point and d is the minimum clearance within the local window. Let T_i^{CP} and T_j^{CP} denote the interpolated arrival indices:

$$\tau = |T_i^{\mathrm{CP}} - T_j^{\mathrm{CP}}|, \qquad d = \min_{t \in \mathcal{W}} \mathrm{dist}!\left(\mathcal{B}_i(t), \mathcal{B}_j(t)\right), \tag{1}$$

where $\mathcal{B}_i(t)$ and $\mathcal{B}_j(t)$ are oriented bounding boxes. Clearance is set to zero when the boxes overlap. Temporal quantities are measured in frames at the SinD sampling frequency.

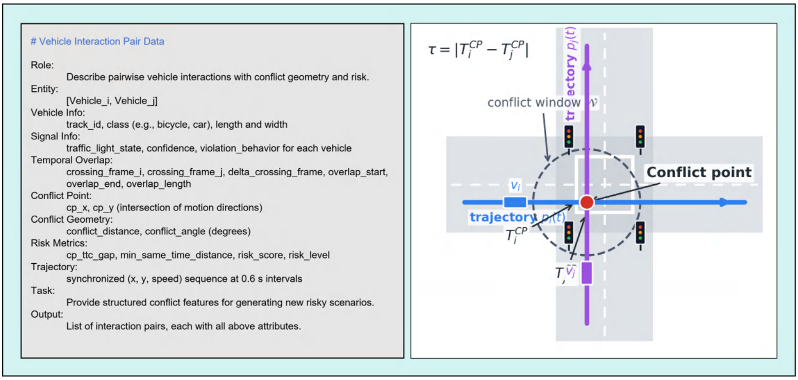

Fig. 2: Interaction representation and conflict geometry. The conflict point is obtained from the recorded paths, and temporal and spatial margins are evaluated within a local window $\mathcal{W}$.

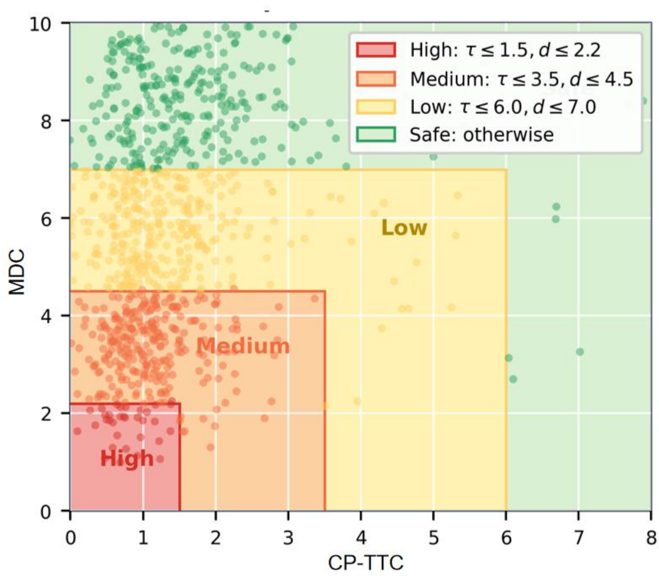

Fig. 3: Empirical levels defined by joint thresholds on the conflict point arrival gap τ and minimum distance clearance d.

A small τ indicates nearly simultaneous access to the conflict region, while a small d indicates limited physical separation. Their joint organization is shown in Fig. 3, where the lower left region represents interactions that are close in both time and space. This compact state supports direct modeling of temporal and spatial safety margins.

For descriptive analysis, interactions are divided into four empirical levels $r \in \{0, 1, 2, 3\}$. The continuous operational score is

$$S_{\text{risk}} = \frac{1}{\tau + 0.25} + \frac{1}{d + 0.50}. \tag{2}$$

This score is a surrogate rather than an accident probability and is used to weight observed interactions during risk field estimation. The discrete levels summarize the state space, while the actual evolution remains continuous.

3.2 Phase Conditioned Risk Potential

After clipped minimum and maximum normalization, $\bar{z} = [\bar{\tau}, \bar{d}]^\top \in [0, 1]^2$. For phase Σ, let $\mathcal{D}_\Sigma$ denote its sample subset and w_k the normalized score from Eq. (2). The empirical component is estimated by

$$\Phi_\rho^\Sigma(\bar{z}) = \frac{\sum_{k \in \mathcal{D}_\Sigma} K_H(\bar{z} - \bar{z}_k) w_k}{\sum_{k \in \mathcal{D}_\Sigma} K_H(\bar{z} - \bar{z}_k) + \epsilon}. \tag{3}$$

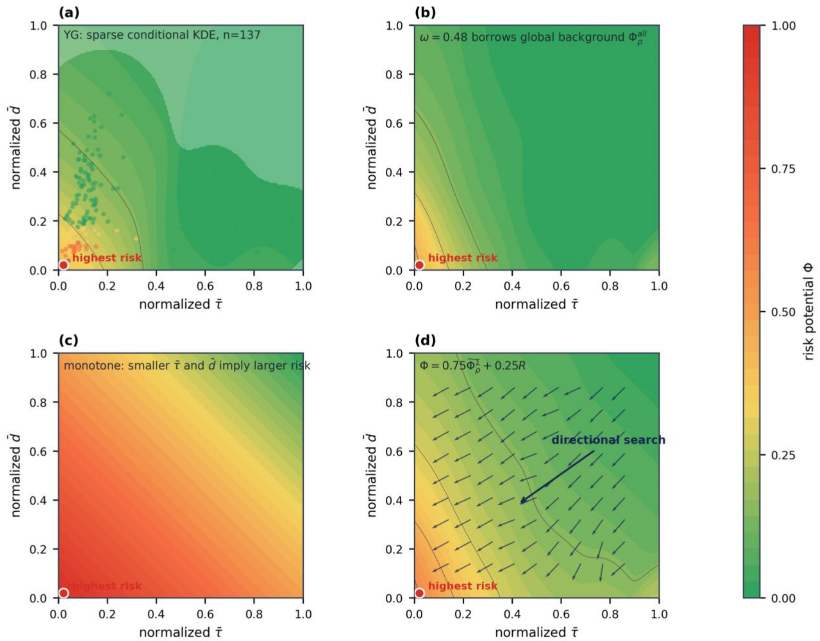

Fig. 4: Construction of the conditional potential from the phase specific estimate, the shrinkage estimate, the structural prior, and the fused potential with characteristic directions.

To reduce variance in sparse phases, phase specific estimates are shrunk toward the global field and combined with $R(\bar{z}) = \frac{1}{2}(1-\bar{\tau}) + \frac{1}{2}(1-\bar{d})$:

$$\widetilde{\Phi}_{\rho}^{\Sigma}(\bar{z}) = \omega_{\Sigma}\Phi_{\rho}^{\Sigma}(\bar{z}) + (1-\omega_{\Sigma})\Phi_{\rho}^{\text{all}}(\bar{z}), \tag{4}$$

$$\Phi(\bar{z} \mid \Sigma) = \lambda_{\rho}\widetilde{\Phi}_{\rho}^{\Sigma}(\bar{z}) + \lambda_R R(\bar{z}), \tag{5}$$

where $\omega_{\Sigma} = n_{\Sigma}/(n_{\Sigma}+\kappa)$, $n_{\Sigma} = |\mathcal{D}_{\Sigma}|$, $\lambda_{\rho} = 0.75$, and $\lambda_R = 0.25$. The analytical term provides a structural bias rather than a strict monotonicity constraint. The fused potential therefore remains stable when phase specific data are sparse.

Fig. 4 shows the effect of each component. Shrinkage suppresses unsupported local peaks, while the structural prior favors smaller margins. The fused field preserves supported phase variation and yields coherent characteristic directions.

3.3 Liouville Characteristic Flow

Let $\rho_s(\bar{z} \mid \Sigma)$ denote a hypothetical population density at the artificial evolution coordinate s. Define

$$v_{\Sigma}(\bar{z}) = \frac{\nabla_{\bar{z}}\Phi(\bar{z} \mid \Sigma)}{|\nabla_{\bar{z}}\Phi(\bar{z} \mid \Sigma)| * 2 + \epsilon_v}, \qquad \frac{\partial \rho_s}{\partial s} + \nabla * \bar{z}! \cdot (\rho_s v_{\Sigma}) = 0. \tag{6}$$

The continuity equation is used only as a population level interpretation and is not solved numerically. Individual states follow $d\bar{z}_s/ds = v_{\Sigma}(\bar{z}_s)$. Along an ideal characteristic,

$$\frac{d\Phi(\bar{z}_s \mid \Sigma)}{ds} = \frac{|\nabla_{\bar{z}}\Phi(\bar{z}_s \mid \Sigma)| * 2^2}{|\nabla * \bar{z}\Phi(\bar{z}_s \mid \Sigma)|_2 + \epsilon_v} \geq 0. \tag{7}$$

Thus, the potential does not decrease along the ideal flow, although both coordinates need not decrease simultaneously. The discrete realization approximates this flow and uses the characteristic field as a direction toward more critical states.

3.4 Path Constrained Trajectory Realization

Candidates are generated by temporally reparameterizing vehicles along their recorded paths. This changes vehicle timing while preserving path geometry. Let $\Delta\tau = \tau^{\text{src}} - \tau^{\text{cand}}$, $\Delta d = d^{\text{src}} - d^{\text{cand}}$, and $\Delta\Phi = \Phi(\bar{z}^{\text{cand}} \mid \Sigma) - \Phi(\bar{z}^{\text{src}} \mid \Sigma)$. Candidates are ranked by

$$\mathcal{L} = -\lambda_{\Phi}\Delta\Phi - \lambda_{\tau}\Delta\tau - \lambda_d\Delta d - \lambda_{\text{align}}\mathcal{A} + \lambda_{\text{cons}}\mathcal{P}_{\text{cons}} + \lambda_{\text{motion}}\mathcal{P}_{\text{motion}}. \tag{8}$$

Here, $\mathcal{A}$ measures alignment with $v_{\Sigma}(\bar{z}^{\text{src}})$, while the penalties discourage excessive source deviation and implausible motion. Lower values are preferred. The selected candidate increases criticality while remaining consistent with the source scene and plausible vehicle motion.

Table 1: Trajectory consistency between source and generated variants.

Metric	Value
ED	7.0934
FD	16.8669
DTW	2.9462

4 Experiments

4.1 Experimental Setup

We evaluate the framework on signal aware interactions from SinD. Each sample contains two vehicles whose paths intersect at a conflict point and whose signal states belong to RR, RG, or YG. The interaction is represented by τ, d, and $\Phi(\bar{z} \mid \Sigma)$. For each source pair, 500 variants are generated and ranked using Eq. (8); the highest ranked feasible candidate is selected. Temporal quantities are reported in frames and seconds at 10 Hz. Evaluation considers path and maneuver preservation, reduction of temporal and spatial margins, and physical realization of state migration.

4.2 Trajectory Consistency

Trajectory consistency indicates whether a generated variant preserves the identity of the recorded scenario. Road geometry, vehicle routes, maneuver classes, and the conflict point are retained because each vehicle remains on its recorded path. Only temporal progress is modified.

We measure deviation using Euclidean distance (ED), Fréchet distance (FD), and dynamic time warping (DTW), where lower values indicate greater consistency. ED measures positional deviation at corresponding frames, FD captures the largest curve discrepancy, and DTW allows nonlinear temporal alignment.

Table. 1 reports ED, FD, and DTW values of 7.0934, 16.8669, and 2.9462. These values quantify the adjustment needed to obtain a more critical interaction while preserving the original paths. They are not protocol independent measures of realism.

Gu et al. [20] report the same metric families for SinD based generation, but their method replaces individual traffic participants with learned GAIL or OF T GAIL agents. Our evaluation measures deviations between recorded interaction pairs and their path constrained variants. Because the objectives, populations, sequence construction, and metric aggregation differ, the values are not directly comparable. As shown in Tab. 2, the two approaches address complementary objectives.

4.3 Risk State Evolution

A reduction in τ means that the vehicles reach the conflict region closer in time, while a reduction in MDC indicates a smaller spatial margin. As reported

Table 2: Methodological comparison with SinD based intersection scenario generation.

Method	Target	Path handling	Signal use	Risk control
OF T GAIL [20]	TP behavior	Frenet reference	Model input	No
Ours	Interaction timing	Fixed source path	Conditional field	Yes

Table 3: Evolution of surrogate interaction quantities.

Metric	Value
Arrival gap reduction ratio	0.7712
MDC reduction ratio	0.9407
Potential increase ratio	0.9831

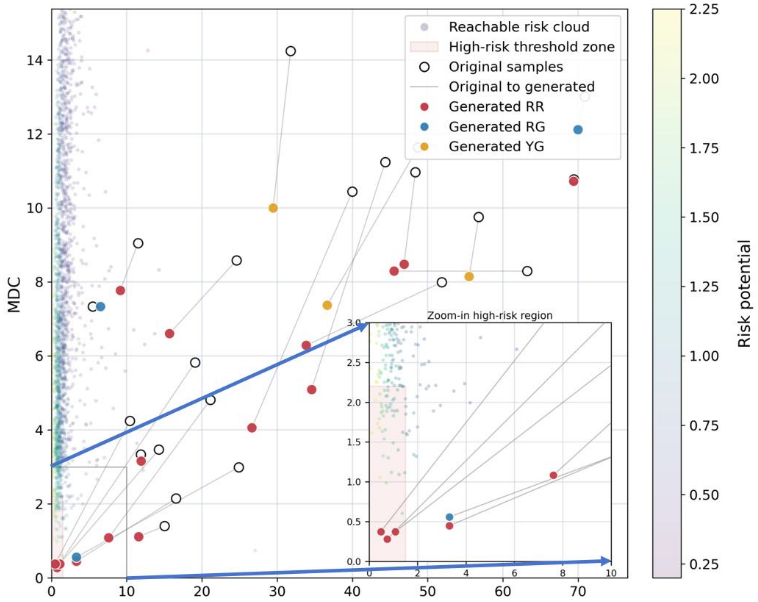

Fig. 5: Signal conditioned risk state transitions from recorded interactions to generated variants.

in Tab. 3, 77.12% of the selected variants reduce τ, and 94.07% reduce MDC. At 10 Hz, the mean reductions are 0.800 s and 2.7073 m, respectively. The conditional potential increases in 98.31% of cases. Because this potential also appears in candidate ranking, the ratio indicates objective consistency rather than collision likelihood.

Fig. 5 shows that most interactions move leftward, downward, or toward the lower left region, indicating reduced temporal separation, reduced spatial clearance, or both. Fig. 6 shows a corresponding population shift toward smaller margins and higher potential. Not every sample decreases both coordinates be-

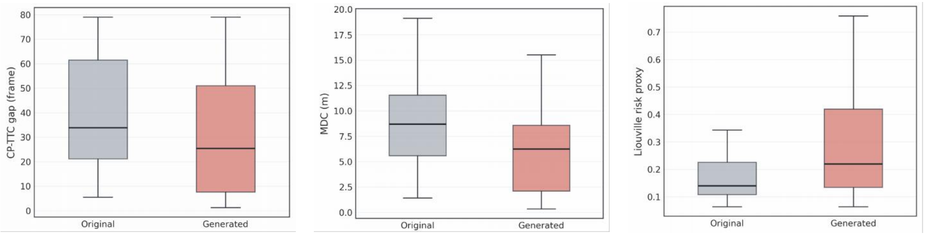

Fig. 6: Distributions of the conflict point arrival gap, minimum distance clearance, and conditional potential before and after evolution.

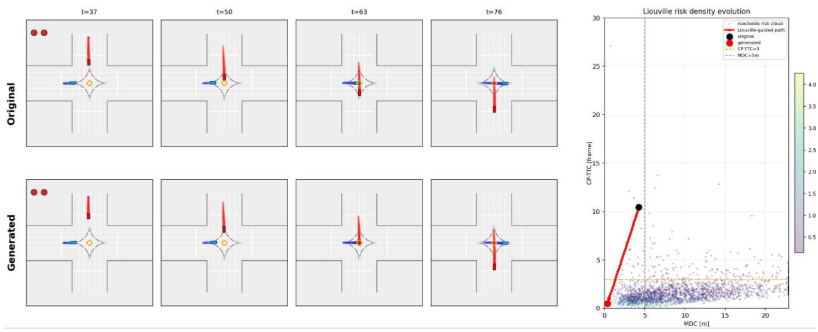

Fig. 7: Qualitative comparison between a source interaction and its generated variant. The spatial paths and maneuver classes are preserved, while temporal progress near the conflict point is resynchronized. The right panel relates this change to the corresponding displacement in risk space.

cause ranking also considers field alignment, trajectory consistency, and motion plausibility.

4.4 Physical Interpretation of Trajectory Evolution

Fig. 7 compares a source interaction with its generated variant. The vehicles retain their original lanes, maneuver classes, and conflict point, while their progress near the intersection becomes more synchronized. The variant therefore represents the same interaction under a less favorable arrival relationship.

In Fig. 7, the arrival gap decreases from 1.655 s to 0.332 s, and the MDC decreases from 2.15 m to 0.45 m. The increased criticality results from greater overlap in conflict region occupancy rather than from route changes or artificial collision geometry. The characteristic field specifies a direction of higher potential, and temporal reparameterization realizes this direction along the recorded paths.

4.5 Discussion

The framework evolves recorded interactions rather than generating unrestricted traffic scenes. Each variant remains traceable to its source, while criticality is increased through controlled timing changes. This supports scenario library expansion, construction of near critical variants, and sensitivity analysis of planning and decision algorithms. Stronger temporal or spatial terms emphasize arrival synchronization or reduced clearance, while larger consistency and motion penalties preserve more source behavior but limit attainable criticality.

Future work can incorporate calibrated conflict labels, simulation outcomes, and closed loop responses to relate surrogate states to collision probability and severity. Adding vehicle dynamics and traffic rules could produce executable trajectories with validated motion profiles. Evaluation across more intersections and signal configurations would test transferability. The pairwise formulation could also be extended to reactive simulations with multiple agents.

5 Conclusion

We presented a signal aware framework that evolves recorded traffic interactions toward more critical states through a phase conditioned potential and path constrained temporal reparameterization. Experiments on SinD show that the generated variants preserve routes, maneuver semantics, and conflict geometry while reducing temporal and spatial margins. Specifically, 77.12% reduce the arrival gap, 94.07% reduce minimum clearance, and 98.31% increase the conditional potential. The results show that criticality is increased through controlled resynchronization rather than spatial path deformation. The method therefore provides traceable and interpretable variants for critical scenario library expansion and autonomous driving system testing.

Acknowledgements

This work was supported by the National Natural Science Foundation of China (62373163), the Natural Science Foundation of Hunan Province (2025JJ60349), and the Science and Technology Research Project of the Education Department of Jilin Province (JJKH20261263KJ).

References

1. Wang, J., Pun, A., Tu, J., Manivasagam, S., Sadat, A., Casas, S., Ren, M., Urtasun, R.: AdvSim: Generating safety-critical scenarios for self-driving vehicles. In: Proceedings of the IEEE/CVF Conference on Computer Vision and Pattern Recognition. pp. 9909–9918 (2021)
2. Arun, A., Haque, M.M., Washington, S., Sayed, T., Mannering, F.: A systematic review of traffic conflict-based safety measures with a focus on application context. Analytic Methods in Accident Research **32**, 100185 (2021)
3. Suo, S., Regalado, S., Casas, S., Urtasun, R.: TrafficSim: Learning to simulate realistic multi-agent behaviors. In: Proceedings of the IEEE/CVF Conference on Computer Vision and Pattern Recognition. pp. 10400–10409 (2021)

4. Jiang, C., Cornman, A., Park, C., Sapp, B., Zhou, Y., Anguelov, D.: MotionDiffuser: Controllable multi-agent motion prediction using diffusion. In: Proceedings of the IEEE/CVF Conference on Computer Vision and Pattern Recognition. pp. 9644–9653 (2023)
5. Li, Q., Peng, Z., Feng, L., Zhang, Q., Xue, Z., Zhou, B.: MetaDrive: Composing diverse driving scenarios for generalizable reinforcement learning. IEEE Transactions on Pattern Analysis and Machine Intelligence **45**(3), 3461–3475 (2023)
6. Xu, Y., Shao, W., Li, J., Yang, K., Wang, W., Huang, H., Lv, C., Wang, H.: SIND: A drone dataset at signalized intersection in china. In: IEEE International Conference on Intelligent Transportation Systems. pp. 2471–2478 (2022)
7. Westhofen, L., Neurohr, C., Koopmann, T., Butz, M., Schütt, B., Utesch, F., Neurohr, B., Gutenkunst, C., Böde, E.: Criticality metrics for automated driving: A review and suitability analysis of the state of the art. Archives of Computational Methods in Engineering **30**(1), 1–35 (2023)
8. Sarkar, D.R., Rao, K.R., Chatterjee, N.: A review of surrogate safety measures on road safety at unsignalized intersections in developing countries. Accident Analysis & Prevention **195**, 107380 (2024)
9. Wang, X., Shi, R., Leich, A., Saul, H., Sohr, A., Bei, X.: Conflict extraction and characteristics analysis at signalized intersections using trajectory data. International Journal of Transportation Science and Technology (2025)
10. Zhou, Z., Wang, J., Li, Y.H., Huang, Y.K.: Query-centric trajectory prediction. In: Proceedings of the IEEE/CVF Conference on Computer Vision and Pattern Recognition. pp. 17863–17873 (2023)
11. Seff, A., Cera, B., Chen, D., Ng, M., Zhou, A., Nayakanti, N., Refaat, K.S., Al-Rfou, R., Sapp, B.: MotionLM: Multi-agent motion forecasting as language modeling. In: Proceedings of the IEEE/CVF International Conference on Computer Vision. pp. 8579–8590 (2023)
12. Huang, Z., Liu, H., Lv, C.: GameFormer: Game-theoretic modeling and learning of transformer-based interactive prediction and planning for autonomous driving. In: Proceedings of the IEEE/CVF International Conference on Computer Vision. pp. 3903–3913 (2023)
13. Wen, D., Xu, H., He, Z., Wu, Z., Tan, G., Peng, P.: Density-adaptive model based on motif matrix for multi-agent trajectory prediction. In: Proceedings of the IEEE/CVF Conference on Computer Vision and Pattern Recognition. pp. 14822–14832 (2024)
14. Yan, Z., Li, P., Fu, Z., Xu, S., Shi, Y., Chen, X., Zheng, Y., Li, Y., Liu, T., Li, C., Luo, N., Gao, X., Chen, Y., Wang, Z., Shi, Y., Huang, P., Han, Z., Yuan, J., Gong, J., Zhou, G., Zhao, H., Zhao, H.: INT2: Interactive trajectory prediction at intersections. In: Proceedings of the IEEE/CVF International Conference on Computer Vision. pp. 8536–8547 (2023)
15. Pronovost, E., Ganesina, M.R., Hendy, N., Wang, Z., Morales, A., Wang, K., Roy, N.: Scenario diffusion: Controllable driving scenario generation with diffusion. In: Advances in Neural Information Processing Systems. vol. 36, pp. 68873–68894 (2023)
16. Xia, J., Xu, C., Xu, Q., Wang, Y., Chen, S.: Language-driven interactive traffic trajectory generation. In: Advances in Neural Information Processing Systems. vol. 37, pp. 77831–77859 (2024)
17. Zhou, Z., Hu, H., Chen, X., Wang, J., Guan, N., Wu, K., Li, Y.H., Huang, Y.K., Xue, C.J.: BehaviorGPT: Smart agent simulation for autonomous driving with next-patch prediction. In: Advances in Neural Information Processing Systems. vol. 37, pp. 79597–79617 (2024)

18. Li, Q., Peng, Z., Feng, L., Liu, Z., Duan, C., Mo, W., Zhou, B.: ScenarioNet: Open-source platform for large-scale traffic scenario simulation and modeling. In: Advances in Neural Information Processing Systems. vol. 36, pp. 3894–3920 (2023)
19. Zhang, J., Xu, C., Li, B.: ChatScene: Knowledge-enabled safety-critical scenario generation for autonomous vehicles. In: Proceedings of the IEEE/CVF Conference on Computer Vision and Pattern Recognition. pp. 15459–15469 (2024)
20. Gu, X., Wu, S., Zhao, S., Zhang, T., Li, X., Jiao, X., Wang, H.: Generation of signalized intersection test scenarios based on traffic participant model. Automotive Innovation **8**, 882–895 (2025)
21. Ljungbergh, W., Tonderski, A., Johnander, J., Caesar, H., Åström, K., Felsberg, M., Petersson, C.: NeuronCAP: Photorealistic closed-loop safety testing for autonomous driving. In: European Conference on Computer Vision. pp. 161–177 (2024)